SCIENCE CHINA
Chemistry

•REVIEWS•

March 2021 Vol.64 No.3: 341–357
https://doi.org/10.1007/s11426-020-9901-4

Recent progress of electronic materials based on 2,1,3-benzothiadiazole and its derivatives: synthesis and their application in organic light-emitting diodes

Youming Zhang[1,2,3], Jun Song[4*], Junle Qu[4], Peng-Cheng Qian[5*] & Wai-Yeung Wong[1,2*]

[1]*Department of Applied Biology and Chemical Technology and Research Institute for Smart Energy, The Hong Kong Polytechnic University (PolyU), Hung Hom, Hong Kong, China;*
[2]*PolyU Shenzhen Research Institute, Shenzhen 518057, China;*
[3]*College of Materials Science and Engineering, Shenzhen University, Shenzhen 518060, China;*
[4]*Key Laboratory of Optoelectronic Devices and Systems of Ministry of Education and Guangdong Province, College of Physics and Optoelectronic Engineering, Shenzhen University, Shenzhen 518060, China;*
[5]*Key Laboratory of Environmental Functional Materials Technology and Application of Wenzhou City, Institute of New Materials & Industry, College of Chemistry & Materials Engineering, Wenzhou University, Wenzhou 325035, China*

Received September 29, 2020; accepted November 2, 2020; published online December 28, 2020

2,1,3-Benzothiadiazole (BT) and its derivatives are very important acceptor units used in the development of photoluminescent compounds and are applicable for the molecular construction of organic light-emitting diodes, organic solar cells and organic field-effect transistors. Due to their strong electron-withdrawing ability, construction of molecules with the unit core of BT and its derivatives can usually improve the electronic properties of the resulting organic materials. In this contribution, we review the synthesis of various polymers, small molecules and metal complexes with BT and its derivatives and their applications in organic light-emitting diodes. Furthermore, the molecular design rules based on these cores are discussed.

2, 1, 3-benzothiadiazole, organic light-emitting diodes, synthesis, electronic properties, photoluminescence

Citation: Zhang Y, Song J, Qu J, Qian PC, Wong WY. Recent progress of electronic materials based on 2,1,3-benzothiadiazole and its derivatives: synthesis and their application in organic light-emitting diodes. *Sci China Chem*, 2021, 64: 341–357, https://doi.org/10.1007/s11426-020-9901-4

1 Introduction

π-Conjugated compounds are important in organic optoelectronic molecules due to their ability to precisely tune optoelectric properties, such as conductivity, charge-carrier mobility, light absorption and light emission. As a consequence, scientists have made great efforts to design organic compounds with excellent electronic transport properties to meet military and commercial requirements. Among the developed organic optoelectronic π-conjugated molecules, the construction of donor (D)-acceptor (A) structures is one of the most effective strategies to regulate the optoelectronic properties of these materials [1–5]. Their band gap levels and optoelectronic properties can be readily tuned through systematic variation between the D and A units [6]. Furthermore, hybridization of the energy levels between the D and A units can decrease the highest occupied molecular orbital (HOMO) and the lowest unoccupied molecular orbital (LUMO) energy levels, which leads to an unusually small HOMO-LUMO energy separation [7]. Therefore, the selection of D and A units is particularly important to synthesize organic π-conjugated materials with excellent optoelectronic properties.

*Corresponding authors (email: songjun@szu.edu.cn; qpc@wzu.edu.cn; wai-yeung.wong@polyu.edu.hk)

In the early stage, D-A organic compounds were often used with non-conjugated electron-accepting groups, such as cyano [8–12], nitro [13–16], or halogen groups [17,18] as substituents on an aryl subunit or a vinylene unit in the organic backbone. In the last decade, aromatic heterocycles with high HOMO energy levels (E_{HOMO}) have received much attention as stronger and more synthetically accessible acceptors. A variety of heterocyclic acceptors have been studied and covered in a couple of reviews [19–29]. However, only some of them are often used, such as 2,1,3-benzothiadiazole (BT) [30–34], 2*H*-benzo[*d*][1,2,3]triazole [35–37], 3,6-di(thiophen-2-yl)pyrrolo[3,4-*c*]pyrrole-1,4(2*H*,5*H*)-dione [38–43] and (*E*)-3-(2-oxoindolin-3-ylidene)indolin-2-one [44–47]. Among those, BT and its derivatives are promising types of acceptor units, owing to their strong electron-withdrawing property, intense light absorption and good photochemical stability, and are often coupled with a variety of electron-rich groups to form low-bandgap polymers, small molecules and transition metal complexes [30,33,48–52]. According to the rules of chemical aromaticity, BT has five pairs of π electrons and possesses excellent aromaticity [30]. This phenomenon attracts the attention of many researchers. BT derivatives have been applied in various fields such as organic photovoltaics (OPVs), dye-sensitized solar cells (DSSCs), organic field-effect transistors (OFETs), organic light-emitting diodes (OLEDs), and electrochromic devices (ECDs) and their physical and chemical properties have been studied intensively [1–5]. So far, chemists have developed a number of BT-based derivatives with electron-withdrawing units, as shown in Figure 1. These derivatives can enhance their electron-withdrawing properties or expand the π-conjugated structure and aromaticity, thus further improving their optoelectronic properties. Based on the advantages of BT and its derivatives, various optoelectronic functional materials have been developed, with most of them exhibiting excellent performance.

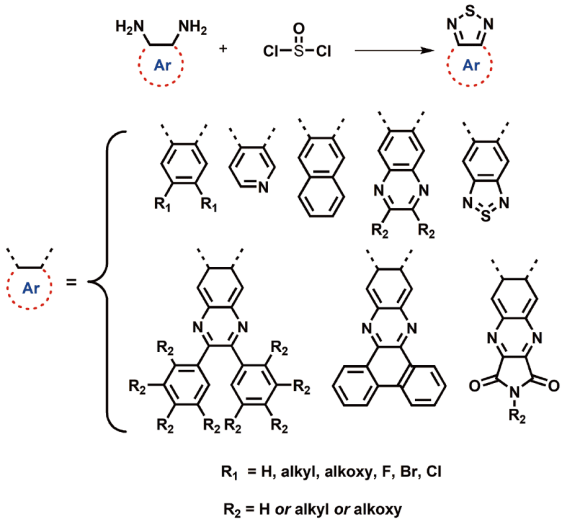

Figure 1 Chemical structures of BT, its derivatives as well as the classical synthetic route (color online).

At present, there are some commercially available BT-based derivative units on the market. However, most of them can only be used in the laboratory for scientific research due to their exorbitant price. Therefore, compounds at lower costs are required to promote commercialization. Optimizing the reaction conditions and reducing the cost of energy are necessary to reduce the price. Based on these considerations, this review summarizes the recent progress on the small molecules, polymers and phosphorescent metal complexes with BT-based units, including their synthesis and application in OLEDs. After a survey on the structural, physicochemical properties and reactivity, the recent advances in the use of BT and its derivatives in OLEDs are disclosed, which are very rare in the literatures. We also discuss the challenges of designing and developing BT-based emitting materials for high-efficiency OLEDs.

2 Synthesis of BT acceptors and their derivatives

In order to combine BT and its derivatives with donor units, some functional groups must be introduced for the synthesis of more BT-containing π-extended photoluminescent compounds. For example, halogen atom can be introduced for the Suzuki coupling reaction [53], tri-*n*-butyltin for the Stille coupling reaction [54] and zinc ion for the Negishi coupling reaction [55]. In these common metal-catalyzed coupling reactions, Suzuki coupling is generally employed as the first choice due to its advantages, including simplicity, mild reaction conditions, good yields and low cost. Hence, 4,7-dibromo-2,1,3-benzothiadiazole (**1**) is the most commonly used intermediate for the synthesis of BT-containing π-extended photoluminescent compounds. A large number of synthetic methods have been reported for this compound. The precursor **1** can be easily prepared in two steps from commercially available *ortho*-phenylenediamine in high yields on multigram and kilogram scales, and the intermediate can then be brominated by using liquid bromine and hydrogen bromide [56–60]. In addition, for regulating the optoelectronic properties of the desired final product, introduction of discrete electron-accepting or -donating substituent groups, such as nitro (**2**) [61], alkoxy (**3**) [62,63], fluoro (**4**) [64] or cyano (**5**) [65] groups, which can weaken or enhance the electron-withdrawing property, into the BT block is considered to be an effective method. Their synthesis steps are generally complex but necessary for improving the performance. Figure 2 shows the synthetic routes of 4,7-dibromo-2,1,3-benzothiadiazole and its discrete substituted derivatives.

Except for the above, some heterocyclic or π-extended thiadiazole derivatives were also developed. For example, 4,7-dibromo-[1,2,5]thiadiazolo[3,4-*c*]pyridine (**6**, Figure 3),

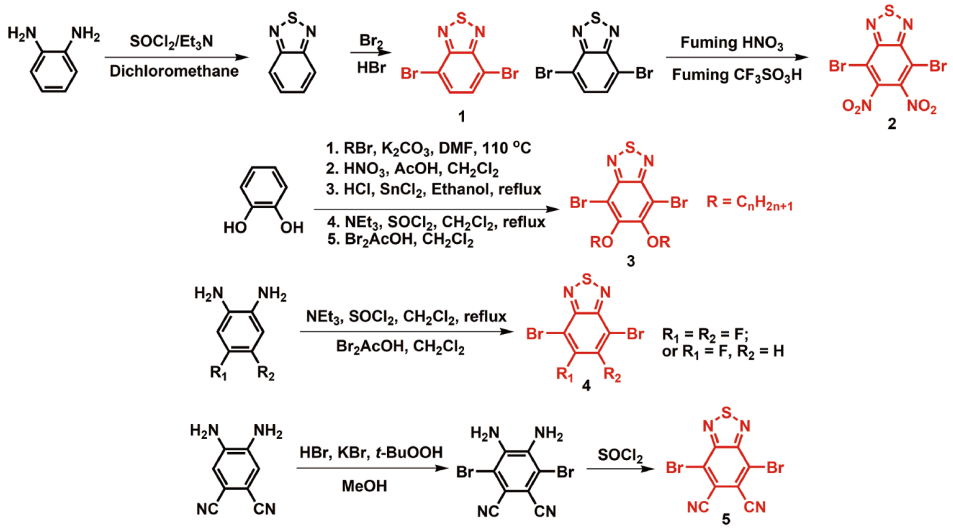

Figure 2 Synthetic routes of 4,7-dibromo-2,1,3-benzothiadiazole and its discrete substituted derivatives (color online).

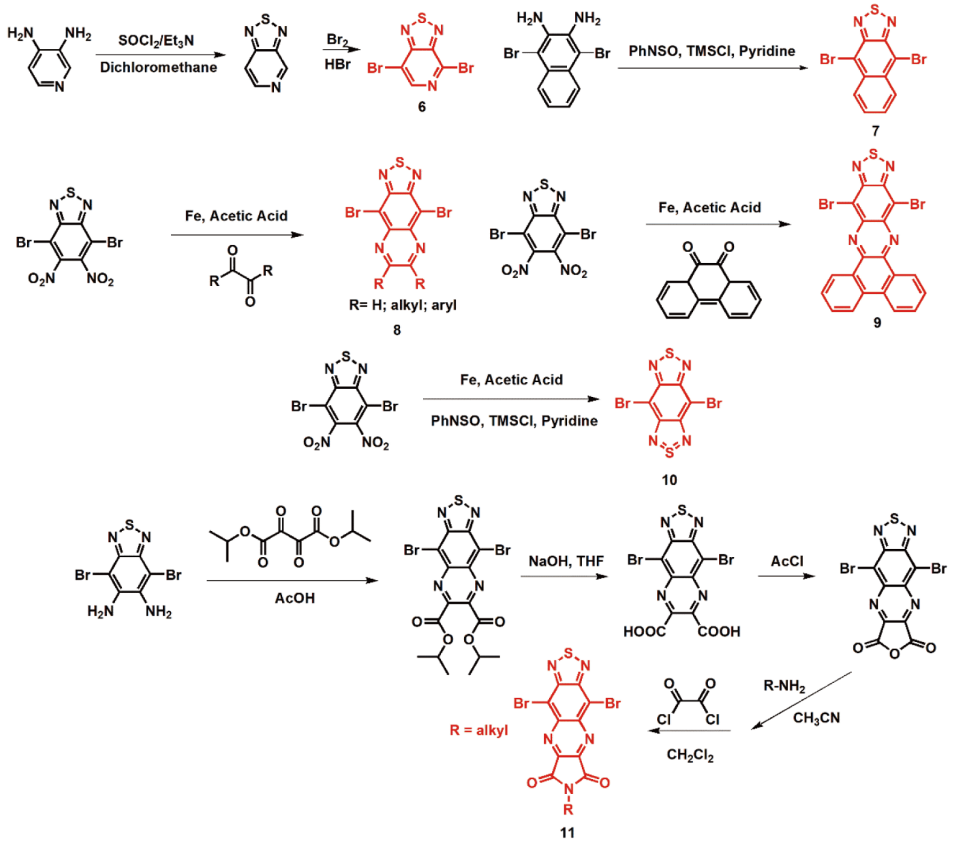

Figure 3 Synthetic routes of benzothiadiazole-containing π-extended electron-deficient units (color online).

which has a strong electron-withdrawing property, can be synthesized by the similar process as 4,7-dibromo-2,1,3-benzothiadiazole when pyridine-3,4-diamine was used as the starting material [66]. Similarly, by further increasing the conjugation of the *o*-aryl diamines or introducing new hetero elements into the heteroaromatic ring, a series of BT-containing π-extended electron-deficient units were reported (**7**–**11**, Figure 3) [67–72]. These units exhibit a broader and stronger absorption ability than BT and have been widely used in the preparation of organic optoelectronic materials, especially for the design of NIR emitting molecules. Furthermore, the BT unit can be transformed into other accep-

tors, such as the quinoxaline derivatives [5].

3 Application in organic light-emitting diodes

Because of their simplified synthesis and excellent light-emitting performance, BT and its derivatives are considered as privileged scaffolds for the production of luminescent organic compounds and are widely applied in different areas of light technology, including OLEDs [30], luminescent probes for analytical and biological applications [73,74], dye-sensitized solar cells, organic photovoltaics and also as wavelength shifting materials [2,24,29]. Among these applications, OLEDs have received particular attention as a strategic technology due to their wide range of applications and have indeed been commercialized. As the core materials of electroluminescent devices, BT and its derivatives are usually used as the emissive-layer materials. Generally, these common organic electroluminescent materials can be in the forms of small molecules, polymers and transition metal complexes. In the following discussion, we summarize the development of these three types of electroluminescent materials containing BT and its derivatives.

3.1 OLED materials based on BT-containing small molecules

Owing to their well-defined molecular structures, ease of purification, amenability to large-scale production and better batch-to-batch reproducibility, small molecule-based OLEDs have received an increasing interest. Early in 2008, Liu *et al.* [75] reported a novel non-planar pentaphenylbenzene-functionalized BT derivative (**12**, Figure 4) and applied it in non-doped OLEDs as a red molecular emitter. This device displayed a red emission with an emission peak at 621 nm, a maximum external quantum efficiency (EQE) of 1% and a maximum brightness of 1,572 cd m^{-2}. Using a BT-based D-π-A bipolar structure as the branching part, three emitter molecules with single, double and triple branched units (**13**–**15**, Figure 4) were fabricated by Li *et al.* [76]. All of these small molecule-based devices showed red emission with an emission peak at 620 nm. Among them, the device based on **13** displayed a maximum luminance of 12,192 cd m^{-2} and a maximum current efficiency (CE_{max}) of 1.66 cd A^{-1}. By using benzothiadiazole-(4-hexyl)thiophene as arms, compounds **16** and **17** (Figure 4) with two arms and three arms, respectively, were further designed and synthesized by Li *et al.* [77]. These two molecules showed red-shifted emission with peaks at 646 and 657 nm. The red-emissive OLED with **17** as the emitting layer and binary poly(*N*-vinylcarbazole) (PVK)/poly-(*N*,*N*′-bis(4-butylphenyl)-*N*,*N*′-bis(phenyl)benzidine) (poly-TPD) as the hole transporting layer (HTL) displayed a high maximum luminance of 7,794 cd m^{-2} and a maximum electroluminescence (EL) efficiency of 0.91 cd A^{-1}, which was among the highest values for the solution-processed red OLEDs at that time. From their optical absorption and photoluminescence (PL) data, there is no or small luminescence peak shift after adding the absorption arms. Hence, the emission peaks mainly originated from the charge transfer between the donor (triphenylamine or thiophene) and the acceptor (BT).

Tang *et al.* [78] synthesized a series of BT-based small molecules for OLED materials. In 2011, they reported three BT and tetraphenylethene-based small molecules **18**–**20** (Figure 5). With the addition of BT and thiophene, the band gaps of these materials were gradually narrowed (2.55 to

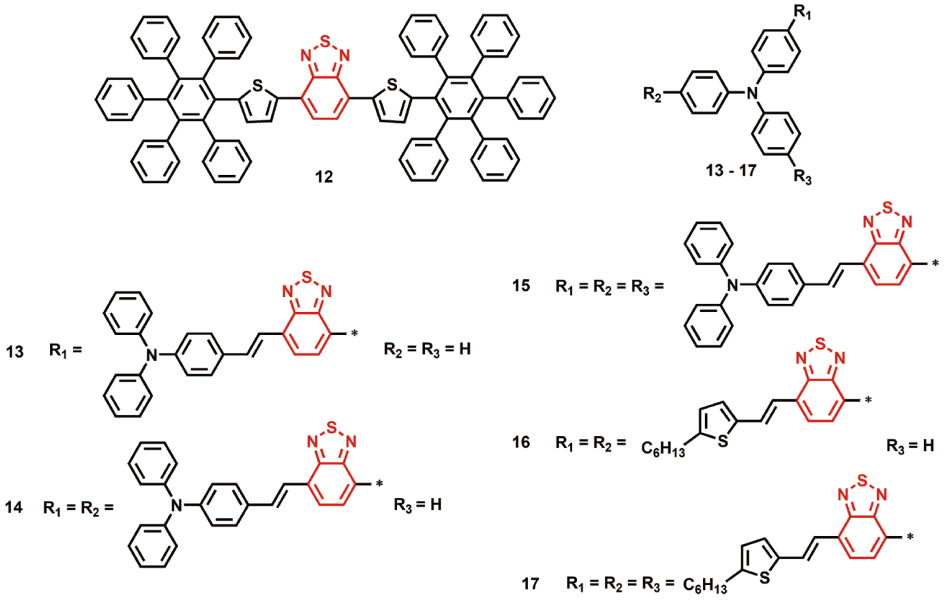

Figure 4 Chemical structures of **12**–**17** (color online).

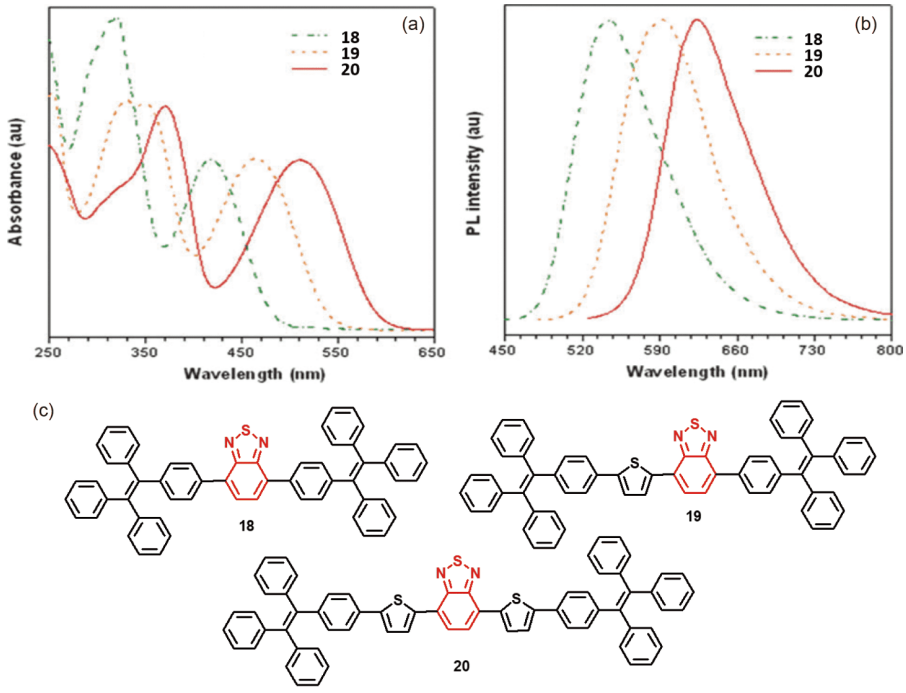

Figure 5 (a) Absorption, (b) PL spectra and (c) chemical structures of **18**–**20**. Adapted with permission [78]. Copyright 2011, The Royal Society of Chemistry (color online).

2.05 eV, **18**–**20**) and exhibited green to red emission (538 to 623 nm). An OLED fabricated using **19** as an emitter exhibited an orange-red EL with high luminance and efficiencies of 8,330 cd m^{-2}, 6.1 cd A^{-1} and 3.1%, respectively. In 2018, Tang's group [79] synthesized three BT-based compounds with tetraphenylethene, phenanthro[9,10-*d*]imidazole and triphenylamine moieties which belong to aggregation-induced emission (AIE) emitters **21**–**23** (Figure 6). The AIE properties can be well modulated by functional groups and *tert*-butyl and diphenylamine moieties are further introduced to modulate the intermolecular interactions and electron donor-acceptor strength. Non-doped OLEDs were fabricated using these red molecules as the light-emitting layers, offering red EL at 650 nm and a high luminance and an EQE of up to 6,277 cd m^{-2} and 2.17%, respectively. Later in the same year, Tang's group [80] further reported another series of BT-based deep red/near infrared (DR/NIR) AIE luminogens **24**–**28** (Figure 6). Their emission wavelengths could be tuned from the red to DR/NIR region by regulating the nature of the substituents. As a result, non-doped OLEDs based on AIEgen **27** showed an EL emission at 684 nm with a large radiance of 5,772 mW Sr^{-1} m^{-2} and an impressive EQE of 1.73%. In order to fully exploit the properties of the material, Kwok *et al.* [81] used **19** as a color conversion cap layer on top-emitting blue OLEDs and white OLEDs (WOLEDs) with Commission Internationale de L'Eclairage (CIE) coordinates of (0.34, 0.35), with high color stability over a wide range of driving voltages and peak efficiencies of 17.7 cd A^{-1} and 8.7 lm W^{-1}.

To further develop efficient luminescent materials, a number of BT-based small molecules have been reported extensively by other research groups for the studies of their structure-property relationships. Promarak *et al.* [82] designed and synthesized three dithienylbenzothiadiazole-derived hole-transporting red emitters **29**–**31** by increasing the number of electron-donating triphenylamine (TPA) functional groups. The absorption and PL spectra of these emitters suggest that introduction of the electron-donating TPA at the donor part of **29** gives rise to more intense intramolecular charge transfer (ICT) interaction in **31** than that in **29**, while adding the electron-donating TPAs at the conjugated backbone of **29** yields less intense ICT interaction in **30** than that in **29** (Figure 7). A simple non-doped red OLED (indium tin oxide (ITO)/poly(3,4-ethylenedioxythiophene) poly(styrenesulfonate) (PEDOT:PSS)/**29** (spin-coated)/2,9-dimethyl-4,7-diphenyl-1,10-phenanthroline (BCP)/LiF-Al) with an efficiency of 6.25 cd A^{-1} at 4.1 mA cm^{-2}, a low turn-on voltage (3.0 V) and a pure red emission (λ_{EL}=656 nm, and CIE=(0.67, 0.33)) was attained. A very simple emitter of **32** based on a benzene-BT-benzene core (Figure 8) was synthesized by Skabara *et al.* [83] and applied in a WOLED device. This molecule possesses a combination of emissive states to give a white light with CIE coordinates of (0.38, 0.45) and a color temperature of 4,500 K. Thomas *et al.* [84] prepared four BT-based materials containing methyl substituents (**33**–**36**, Figure 8). The steric effect exerted by the methyl group is responsible for the non-planar arrangement of donor and acceptor, which inhibits the intramolecular

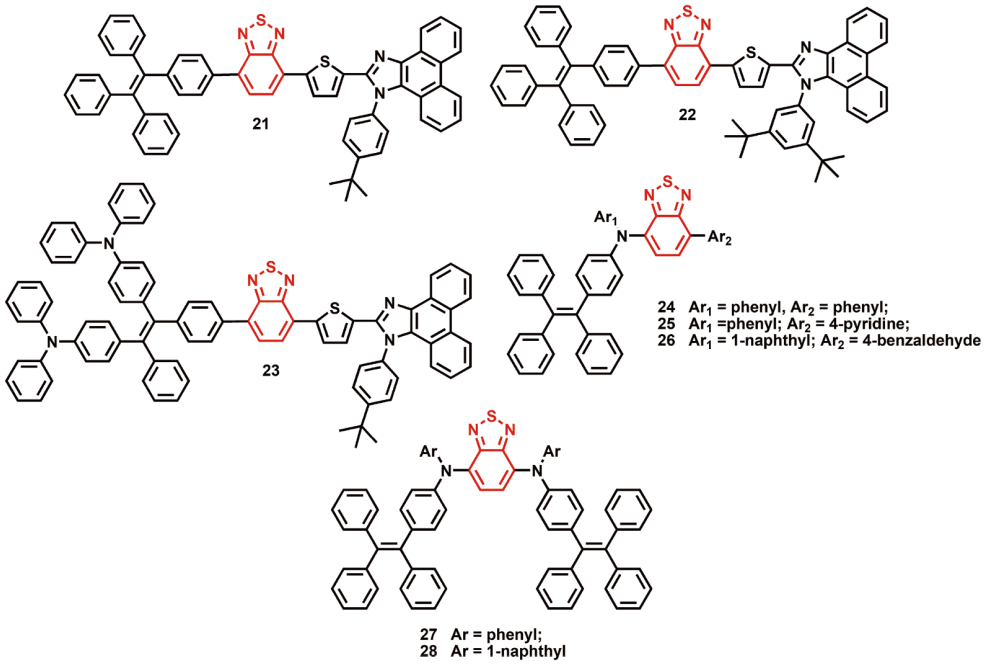

Figure 6 Chemical structures of **21**–**28** (color online).

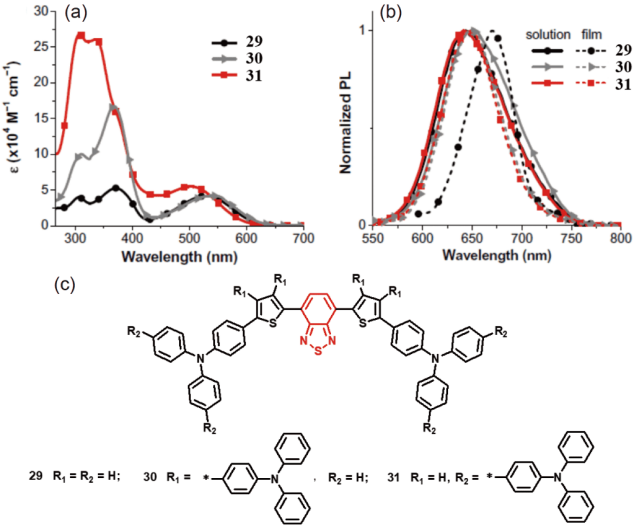

Figure 7 (a) Absorption, (b) PL spectra and chemical structures of **29**–**31**. Adapted with permission [82]. Copyright 2015, Elsevier (color online).

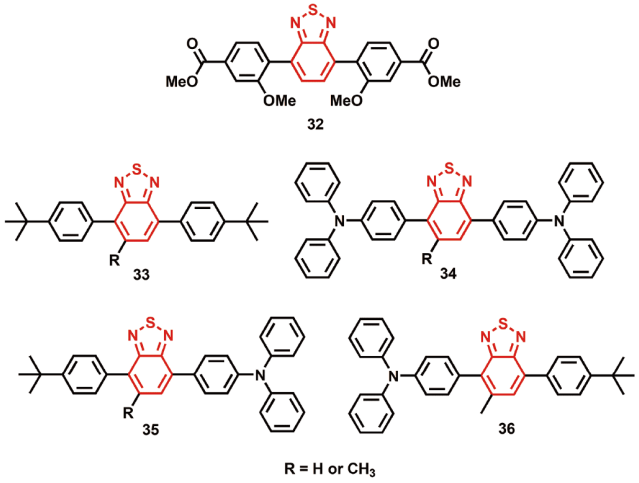

Figure 8 Chemical structures of **32**–**36** (color online).

charge transfer. The emitters exhibited absorption and emission at shorter wavelength when compared to non-methylated emitters. Solution-processed multi-layered OLED devices were fabricated by employing these compounds either as the host or dopant emitter in a suitable host matrix and exhibited green/yellowish green EL with an EQE of 4.6%. With the above investigation, apart from the intramolecular donor-acceptor interaction, the spatial configuration of the molecules also has a great influence on the optical and electrical performance.

Recently, there are some new reports on OLEDs using BT-based small molecules. Lu *et al*. [85] synthesized four D-A-D′ type fluorescent materials by using BT as the acceptor, TPA as the donor, and monocarbaborane (**37**), phenyl (**38**), *p*-methoxyphenyl (**39**) or 4-pyridinyl (**40**) as the terminal donor group (Figure 9). Interestingly, these luminescent materials can aggregate to form nanoparticles or nanocrystals upon adding water to their dilute tetrahydrofuran (THF) solutions. Thus, they can also be applied as chemosensors for silver ion detection. Although the device performance is not good enough to compete with the reported ones, a series of electroluminescent devices with different properties were obtained when these emitters were used as the guest.

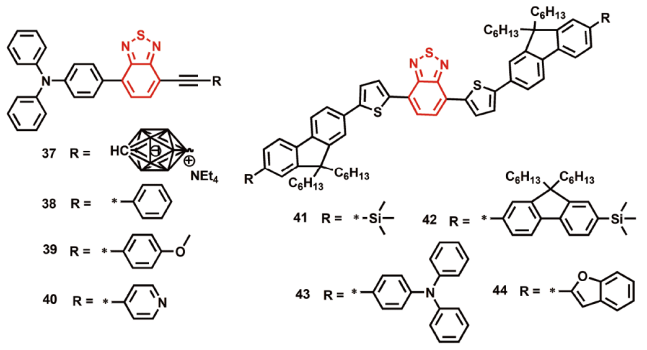

Figure 9 Chemical structures of **37**–**44** (color online).

Moreover, by doping **37** in PVK, a WOLED was obtained, which represented the first example of monocarbaborane-based materials for OLED applications. In order to develop red emitters, Skabara *et al.* [86] also reported four red fluorescent materials based on the fluorene-thiophene-BT motif (**41**–**44**, Figure 9). By extending the molecular conjugation through end-capping with additional fluorene units, or through incorporation of donor functionalities, compounds **42**–**44** exhibited improved OLED performance relative to the parent compound **41**. Although the device performance is not satisfactory, these molecules could also be considered as inexpensive fluorescent orange OLEDs for tandem white light devices.

In recent years, to avoid environmental toxicity, high cost and improve the luminous efficiency, new thermally activated delayed fluorescence (TADF) and hybridized local and charge-transfer state (HLCT) materials have been proposed to harvest both singlet and triplet excitons and break the 5% EQE limit in OLED devices by controlling the excited state with both local excitation (LE) and charge transfer (CT) features and regulating the orbital separation between HOMO and LUMO [87–91]. For TADF, this kind of molecules can use the triplet excitons through RISC from the lowest triplet (T_1) to the lowest singlet states (S_1), resulting in a theoretical internal quantum efficiency of 100%. So, the value of S_1-T_1 energy gap (ΔE_{ST}) is the most important factor for the photophysical and EL properties. The smaller ΔE_{ST} is beneficial for harvesting the triplet excitons *via* reverse intersystem crossing (RISC). For HLCT emission, the intersystem crossing of excitons between T_m and S_n with close energy levels can also occur in the excited state. This state combines both local excited (LE) and charge transfer (CT) states into a special one, possessing two combined and compatible characteristics: a large transition moment from the LE state (cold exciton) and a weakly bound exciton from the CT state (hot exciton). Based on these luminescence mechanisms, scientists have developed many highly efficient BT-based metal-free electrofluorescent emitters.

Yang *et al.* [92] designed and synthesized three D-A-D structured fluorescent molecules by rationally employing BT as an acceptor (**45**–**47**, Figure 10). With an increase in the steric hindrance of the donor moieties (from diphenylamine to 9*H*-carbazole and then to 9,9-dimethyl-9,10-dihydroacridine), the dihedral angles between the donor and acceptor moieties of **45**, **46** and **47** reveal an obvious increase (from 42°, 53° to 61° then to 86°). This spatial configuration can effectively regulate the distribution of HOMO and LUMO energy levels, and thus control the luminescence spectrum (Figure 10). Among them, emitter **47** showed an excellent TADF performance. It is worth mentioning that OLEDs containing the TADF emitter **47** achieved a maximum EQE of 8.8% with the emission peak at 636 nm. Ma *et al.* [93] designed BT-based D-A-type chromophores in **48** (Figure 11). This emitter possesses a non-planar "butterfly-like" structure with a C–S–N–C dihedral angle (θ_N) of 142° and can break the spin statistics to utilize the triplet energy through HLCT. The EQE of the NIR OLED based on **48** was 1.54% with a low efficiency roll-off. The result suggests that

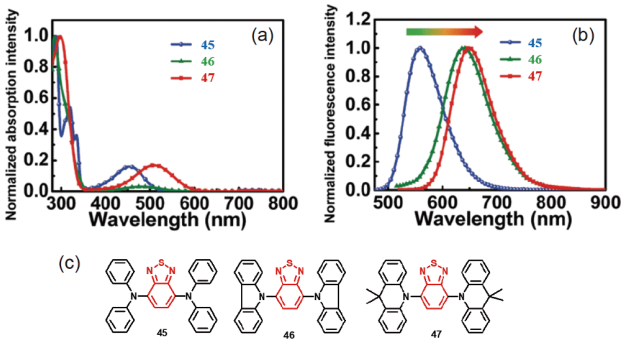

Figure 10 (a) Absorption, (b) PL spectra and (c) chemical structures of **45**–**47**. Adapted with permission [92]. Copyright 2017, The Royal Society of Chemistry (color online).

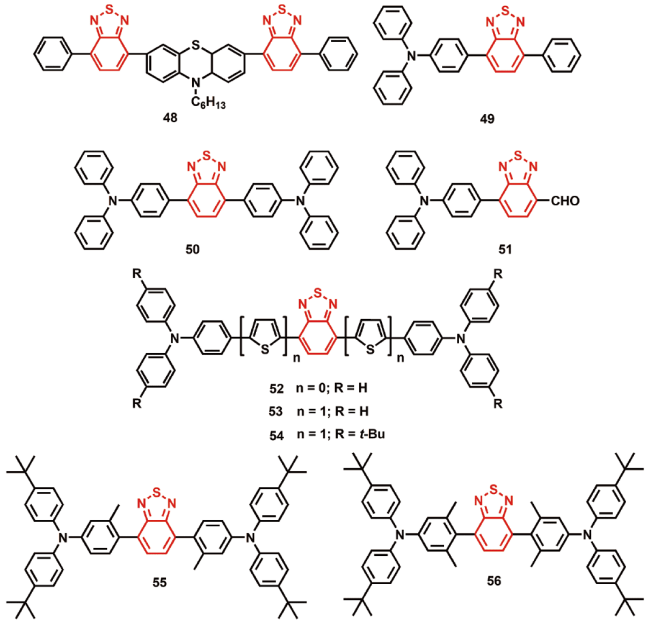

Figure 11 Chemical structures of **48**–**56** (color online).

fluorescent molecule with "hot-exciton" mode and an HLCT state is an ideal strategy to design next-generation, high-efficiency and low-cost OLED materials and brings new hope for the development of organic small-molecule electroluminescent materials. Later, they further developed this concept with BT-based small organic molecules. Among them, the device of BT-based small organic molecule **49** (Figure 11) exhibited an EQE of 3.8% [94]. Chi *et al.* [95] reported two BT-based red fluorophores (**50** and **51**, Figure 11) with HLCT properties. Compounds **50** and **51** enabled nondoped OLEDs with excellent EQE of 11.1% and 5.0%, attributed to the high exciton utilization efficiency of 82% and 46%, Furthermore, dyes **50** and **51** were utilized as complementary emitters with a sky-blue TADF material to fabricate two-color fluorescent WOLEDs in a fully non-doped emissive-layer configuration, and achieved high EQEs of 23.0% and 8.6%, respectively. Su *et al.* [96] prepared three D-A-type emitters with 5,6-difluorobenzo[*c*][1,2,5]thiadiazole as the acceptor, TPA as the donor, and thiophene as the π-bridge (**52**–**54**, Figure 11). These materials can emit orange-yellow to NIR emission due to the insertion of thiophene, and possess HLCT feature which may lead to an exciton utilization exceeding the limit of 25% of traditional fluorescent materials. As a result, the related devices exhibited relatively good performance with maximum EQE of 5.75%, 0.83%, and 1.44% for **52**, **53**, and **54** based OLEDs, respectively. In 2020, Wong's group [97] also reported two BT-based emitters by introducing one or two methyl groups between the donors and acceptor (**55**–**56**, Figure 11). Through the introduction of sterically hindered methyl groups, the spatial configuration of molecules has greatly changed, and thus the overlap of HOMO and LUMO has been effectively regulated. As a result, emitter **55** showed an obvious HLCT feature with high PL quantum yield in organic solvents and solid state. Their corresponding devices showed excellent performances with maximum EQE of 8.47% and 7.29% for **55** and **56** doped OLEDs. Table 1 summarizes the photophysical and EL properties of various BT-containing small molecules.

3.2 OLED materials based on BT-containing polymers

Due to their advantages of better film-forming properties, mechanical strength and thermal stability, as well as being able to fabricate large area electroluminescent devices by spin-coating, conjugated polymers have attracted tremendous attention in the field of flexible and large area optoelectronic devices based on low-cost solution processing techniques. In recent decades, remarkable progress has been realized in the development of new π-conjugated materials for various applications, especially in terms of white light emission in OLEDs. For their simple chemical structures and excellent device performances, polymer electroluminescent

Table 1 Photophysical and EL properties of BT-containing small molecules [a)]

	λ_{PL} (nm)	λ_{EL} (nm)	CE_{max} (cd A^{-1})	PE_{max} (lm W^{-1})	EQE_{max} (%)	Ref.
12	609	621	1.37	–	1.0	[75]
13	643	620	4.76	–	–	[76]
14	643	620	5.39	–	–	[76]
15	643	620	4.69	–	–	[76]
16	646	642	0.53	–	–	[77]
17	657	649	0.91	–	–	[77]
18	538	540	5.2	3.0	1.5	[78]
19	592	592	6.4	2.9	3.1	[78]/[81]
20	623	668	0.4	0.5	1.0	[78]
21	600	650	1.31	1.59	2.17	[79]
22	611	638	1.41	1.70	2.03	[79]
23	642	638	2.19	1.61	2.09	[79]
24	620	–	–	–	–	[80]
25	615	–	–	–	–	[80]
26	625	–	–	–	–	[80]
27	666	684	–	–	1.73	[80]
28	658	682	–	–	1.43	[80]
29	643	675	1.79	1.60	–	[82]
30	641	656	6.25	5.17	–	[82]
31	650	662	4.22	3.16	–	[82]
32	487	580	6.5	2.60	2.39	[83]
33	489/512	–	–	–	–	[84]
34	577/639	560	6.2	11.6	4.5	[84]
35	575/630	548	15.7	12.2	4.6	[84]
36	571	540	15.2	10.9	4.8	[84]
37	564	400/576	0.32	0.20	0.18	[85]
38	593	390/585	0.88	0.64	0.40	[85]
39	581	396/590	0.68	0.51	0.32	[85]
40	603	399/581	0.28	0.15	0.15	[85]
41	620	–	0.30	–	0.28	[86]
42	623	–	0.51	–	0.77	[86]
43	626	–	0.30	–	0.46	[86]
44	623	–	0.16	–	0.25	[86]
45	559	–	–	–	–	[92]
46	638	–	–	–	–	[92]
47	648	636	11.0	10.8	8.0	[92]
48	722	692	–	–	1.54	[93]
49	578/567	588	8.84	7.18	3.8	[94]
50	612	608	17.7	12.4	11.1	[95]
51	638	640	4.7	2.5	5.0	[95]
52	563	–	–	–	–	[96]
53	630	630	5.15	4.27	5.75	[96]
54	645	642	2.98	2.60	4.94	[96]
55	546–710	560	30.40	23.67	8.47	[97]
56	528–670	554	35.02	20.37	7.29	[97]

a) λ_{PL} is the peak wavelength of photoluminescence, and λ_{EL} is the peak wavelength of electroluminescence.

materials based on BT acceptor units show great potential. In 2008, Yang *et al*. [98] reported a ternary fluorene-based copolymer (**57**, Figure 12) with the fluorene segment as a blue emitter and the side chain iridium complex as a red emitter that can realize efficient white light emission. By introducing a fluorescent green BT unit into the polyfluorene backbone, the efficiency and color purity of the ternary co-polymers were improved compared to their binary fluorene-based copolymer without the BT acceptor. Furthermore, the efficiency can be increased by increasing the concentration of the iridium complex, which resulted from its efficient phosphorescence emission and the weak phosphorescent quenching due to its lower triplet energy level than that of polyfluorene. Soon afterwards, the same group synthesized another copolymer (**58**, Figure 12) by incorporating BT and iridium complex units into the polyfluorene backbone by the Suzuki polycondensation [99]. This main-chain polymer showed a similar white emission compared to **57** with a maximum luminous efficiency of 5.3 cd A^{-1} and a maximum luminance of 9,900 cd m^{-2}. By doping a concentration of 0.05 mol% 4,7-bithienyl-2,1,3-benzothiadiazole molecule into the polyfluorene chain as an orange-emitting unit, a type of polyfluorene copolymer (**59**, Figure 12) used for WOLEDs was synthesized by Wang *et al*. [100] in 2013. The Förster energy transfer in an inter-chain was investigated through the change of performance caused by the different annealing temperature. In addition, by regulating the ratio of the BT-based red-emitting monomer in conjugated polymers, Somanathan *et al*. [101] reported a copolymer (**60**, Figure 12) that can emit a white emission in a single layer device. Analyzed from the above case, the white light emission of the polymer is mostly obtained through the charge transfer within the polymer repeating unit, and the emission usually originateds from the single molecule luminescence.

Benefiting from the conjugated push-pull branching unit, multi-arm shaped molecules always exhibit broader and stronger absorption/emission. Chromophores with different colors, such as red, green and blue, can be fused in the same molecule to realize white emission in a single-polymer system. Lai and co-workers [102–104] reported a series of three-, four- and six-armed star-shaped polymers (**61**–**64**, Figure 13) with white light emission based on the BT moiety. Using these star-shaped polymers as single dopants, most of their single-emissive-layer OLEDs demonstrated high-efficiency white light emission. For example, the three-armed star-shaped polymer **64** (Figure 13) exhibited high color quality saturated white EL with a CE_{max} of 2.09 cd A^{-1} and CIE coordinates of (0.34, 0.33), which matched well with the values of standard saturated white emission at (0.33, 0.33). Considering their excellent EL performance, star-shaped polymers could be an important direction for the development of white light emissive materials.

Due to their strong electron-withdrawing property, the BT-based polymers typically exhibit a narrow band gap and can usually emit DR and even NIR emission. For example, Gao *et al*. [105] reported two conjugated polymers (**65** and **66,** Figure 14) by using 5,6-dialkoxy-derived benzothiadiazole derivatives as the dopant. By incorporating another BT unit in the main chain, the highest EQE and luminous efficiency were improved by two orders of magnitude for the new polymer **66**. In addition, Patri *et al*. [106] synthesized a series of low band gap π-conjugated BT-based polymers (**67**–**69**, Figure 14). Because of the D-A interactions within the repeating units, an absorption band in the range of 687–663 nm with a band gap in the range of 1.35–1.43 eV and a PL emission between 755 and 773 nm were observed. Qu *et al*. [107] reported another terpolymer (**70**, Figure 14) containing

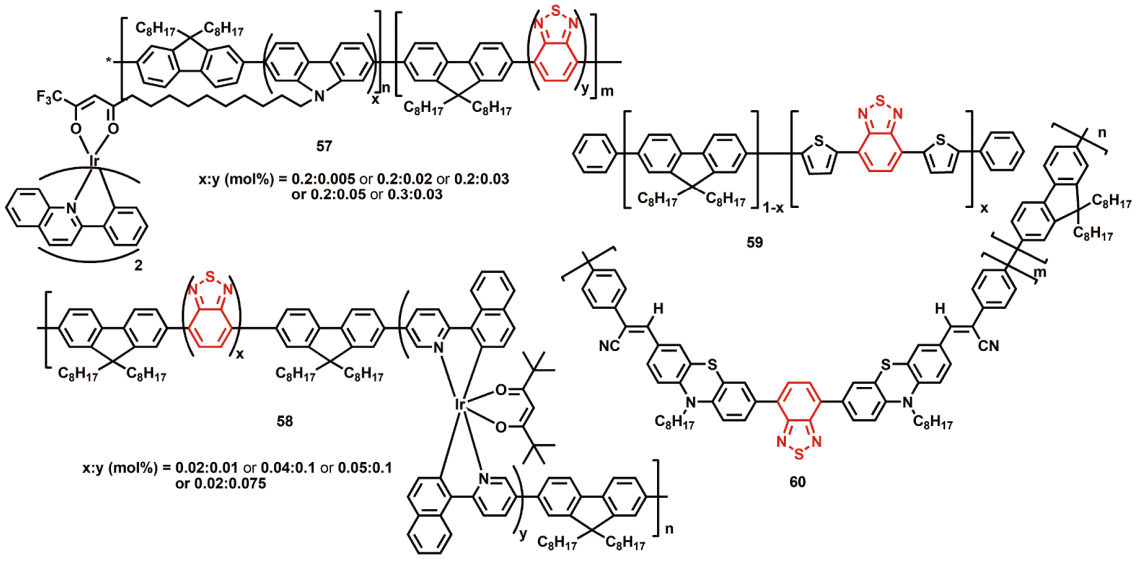

Figure 12 Chemical structures of **57**–**60** (color online).

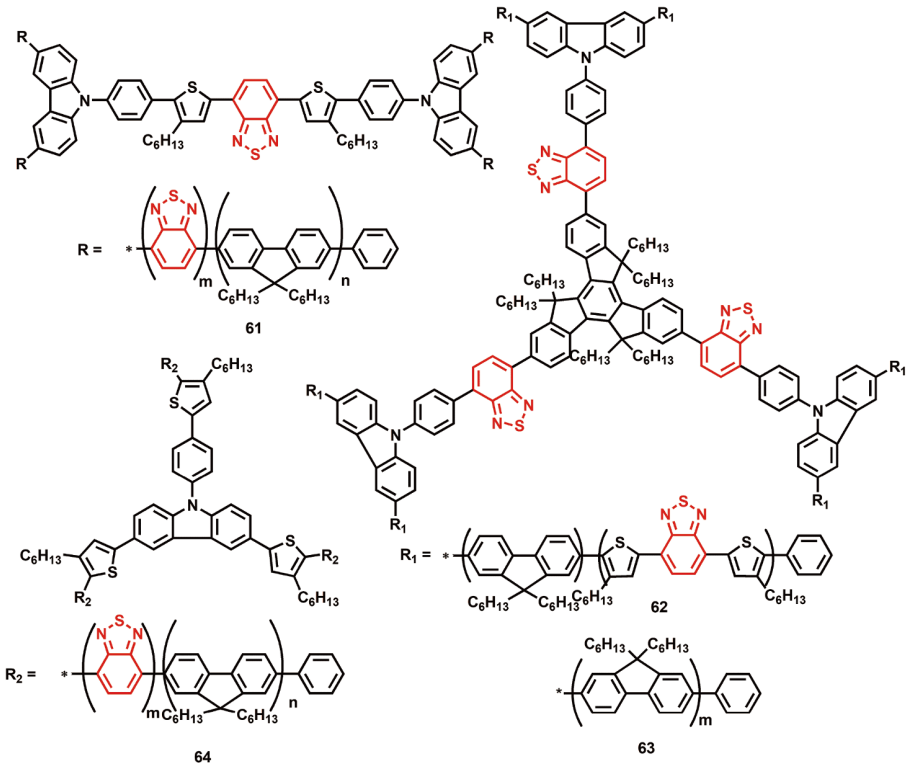

Figure 13 Chemical structures of **61**–**64** (color online).

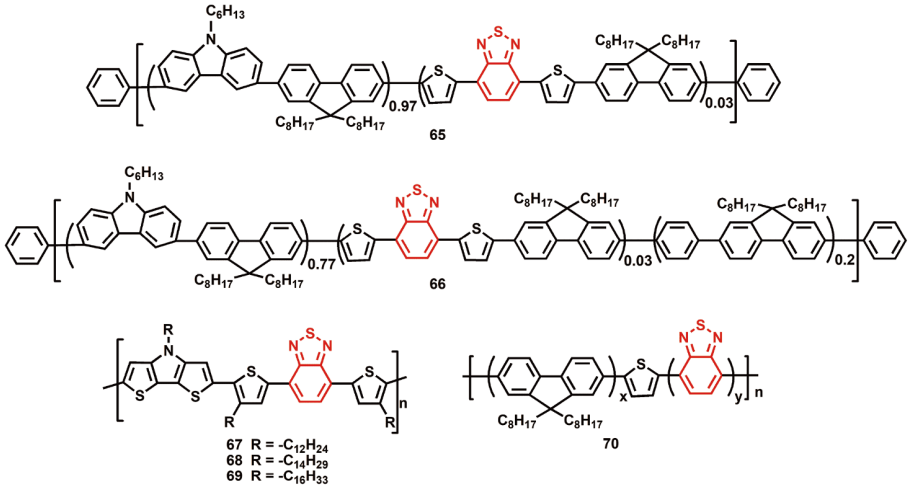

Figure 14 Chemical structures of **65**–**70** (color online).

9,9-dioctylfluorene, thiophene and BT units. A NIR emission device using this polymer as an emitter with an emission peak at 708 nm and luminance of 226 cd m^{-2} was obtained.

The luminescence efficiency of quantum dots can be improved by doping organic polymers into the device. Varlikli *et al*. [108] reported a hybrid polymer light-emitting diode (PLED) containing a BT-based yellow-emitting polymer (**71**, Figure 15) and copper indium disulfide/zinc sulfide as the active layer. This device showed yellow EL with a maximum brightness of 56,834 cd m^{-2}, a CE_{max} of 4.7 cd A^{-1} and a maximum power efficiency (PE_{max}) of 2.3 lm W^{-1}. BT-based polymers also performed well when they were used as the electron/hole transport materials. Woo and co-workers [109] designed and synthesized a BT-based alcohol-soluble conjugated polymer **72** (Figure 15). The resulting device using this polymer as an electron transport material exhibited improved performance compared to an Al cathode-based device and was comparable to the performance of the device with a Ca cathode. For hole transport materials, Grigalevicius *et al*. [110] reported two polyethers containing electro-

active pendant 4-(carbazol-2-yl)-7-arylbenzo[*c*]-1,2,5-thiadiazole moieties (**73** and **74**, Figure 15). These two polyethers showed very high thermal stability with initial thermal degradation and glass transition temperatures. The hole-transporting properties of the polymeric materials were tested in OLEDs with tris(8-hydroxyquinolinato)aluminium (Alq_3) as the green emitter and electron transport material. The device exhibited a turn-on voltage of 6.2 V, a CE_{max} of 2.5 cd A^{-1} and a maximum brightness exceeding 300 cd m^{-2}, which is 30%–90% higher than that of the device containing the widely used hole-transporting layers of poly(9-vinylcarbazole). Table 2 summarizes the photophysical and EL properties of BT-containing polymers.

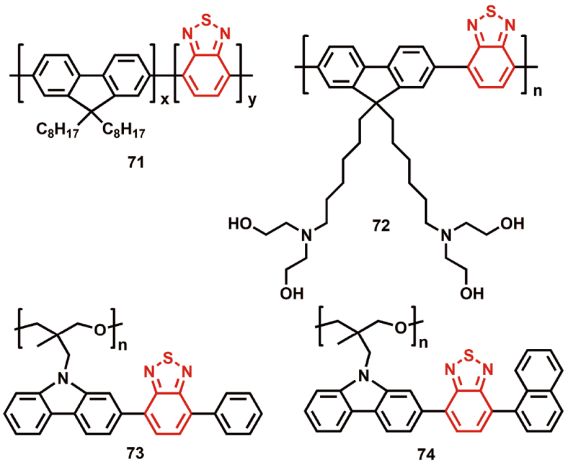

Figure 15 Chemical structures of **71**–**74** (color online).

3.3 OLED materials based on BT-containing transition metal complexes

In comparison to the small molecule- or polymer-based pure organic OLED materials, transition metal complexes can exhibit higher emission efficiency due to their strong spin-orbit coupling in the presence of heavy metals, which leads to an internal quantum efficiency theoretically as high as 100%. In order to investigate the D-A interaction of transition metal complexes and obtain a NIR phosphor, as well as electroluminescent devices, Zhu and co-workers [111–113] reported a series of platinum(II) complexes (**75**–**79**, Figure 16) with NIR phosphorescent emission based on BT-containing ligands. Using these complexes as single dopants, all of their single-emissive-layer OLEDs exhibited high-efficiency NIR emission. Their work strongly proved that appending a D-A framework into a complex is a useful strategy to obtain high-performance NIR emission.

In addition, to further study the structure-property relationships of platinum(II) phosphors, particularly the effect of D-A structure on their photophysical and electronic properties, Wong's group [114] also reported a series of platinum(II) complexes **80**–**83** with an isomeric D-A conjugated BT-based ligand framework (Figure 17). The BT derivative of [1,2,5]-thiadiazolo[3,4-*c*]pyridine was used as the acceptor and coordination unit due to its stronger electron-withdrawing property. These isomeric complexes exhibit PL emissions ranging from 590 to 800 nm with band gaps of 1.7−2.0 eV. OLEDs using these complexes as single emissive layers dis-

Table 2 Photophysical and EL properties of BT-containing polymers

	λ_{PL} (nm)	λ_{EL} (nm)	CE_{max} (cd A^{-1})	PE_{max} (lm W^{-1})	EQE_{max} (%)	Ref.
57	440/580	400–700	6.1	–	–	[98]
58	440/530	420/520/625	5.3	–	2.7	[99]
59	423/446	440/635	3.51	–	–	[100]
60	415/637	528	4.5	4.2	–	[101]
61	–	425/426/517/566	2.74	–	1.1	[102]
62	–	–	1.71	0.68	1.45	[103]
63	–	–	1.60	0.77	1.51	[103]
64	–	430/450/512/600	2.09	–	1.01	[104]
65	579	616	0.006	–	0.008	[105]
66	575	616	1.26	–	1.04	[105]
67	758	795	–	–	–	[106]
68	763	780	–	–	–	[106]
69	773	814	–	–	–	[106]
70	628	708	0.039	–	–	[107]
71	550	–	2.26	1.18	–	[108]
72	539	–	2.40	–	–	[109]
73	–	–	2.5	–	–	[110]
74	–	–	1.5	–	–	[110]

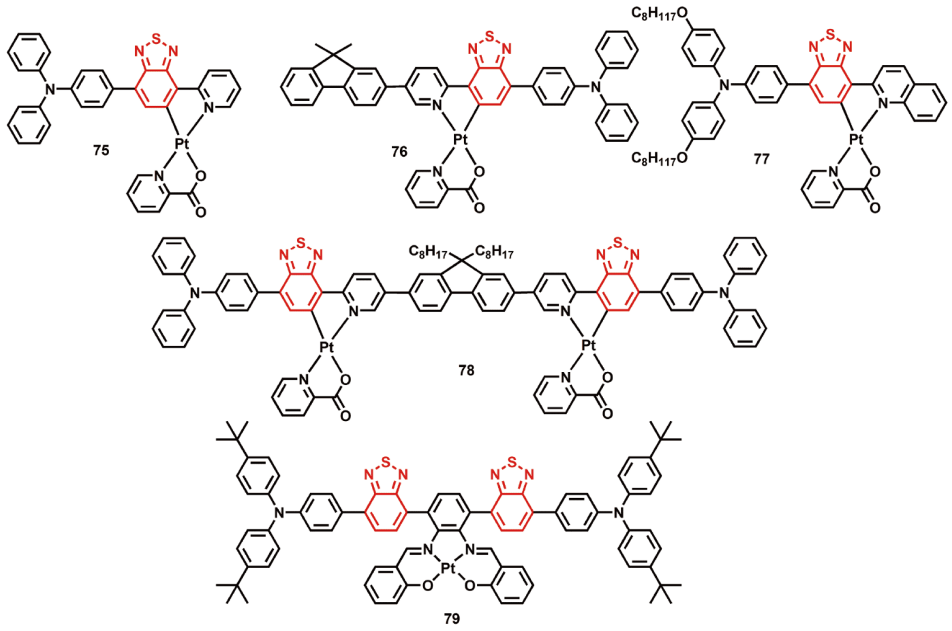

Figure 16 Chemical structures of **75**–**79** (color online).

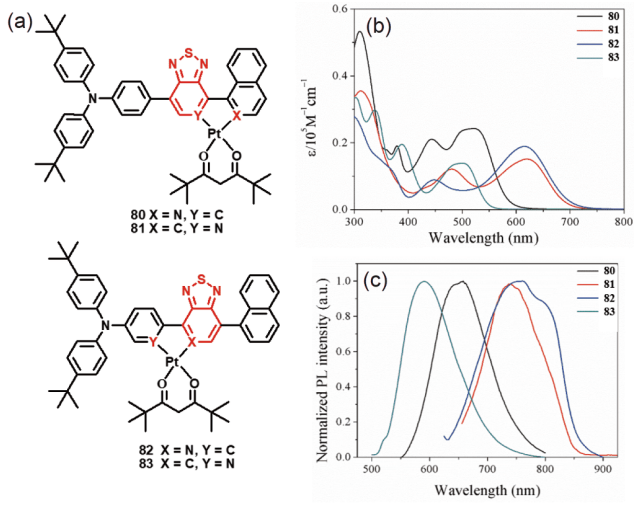

Figure 17 (a) Chemical structures, (b) absorption and (c) PL spectra of **80**–**83**. Adapted with permission [114]. Copyright 2018, American Chemical Society (color online).

play EL peaks at 626, 645, 826 and 571 nm, affording maximum EQEs of 0.13%, 0.04%, 0.49% and 0.22% for **80**–**83** doped devices, respectively. These results indicate that adjusting the coordination position with the isomeric conjugated ligand framework is an appropriate strategy to tune the light-emitting properties of platinum complexes in OLEDs. Table 3 summarizes the photophysical and EL properties of BT-containing transition metal complexes.

3.4 OLED materials based on π-extended BT derivatives

Generally, π-extended BT derivatives have a higher degree of conjugation and stronger electron-deficient ability. The resulting molecules usually exhibit absorptions at long wavelengths and narrower energy band gaps, making them potentially good candidates for NIR-OLEDs. There are many π-extended BT derivative-based small molecules and polymer materials that have been developed for NIR-OLEDs. Early in 2008, Wang and co-workers [115] reported a series of D-π-A-π-D-type NIR fluorescent compounds based on benzobis(thiadiazole) and its selenium analogues (**84**–**94**, Figure 18). The PL wavelength of these chromophores ranges from 900 to 1,600 nm and their band gaps are between 1.19 and 0.56 eV. Interestingly, replacing the sulfur by selenium can lead to a red shift in emission and reduce the band gap further. Using these organic materials as single emissive layers, NIR emissions above 1 μm with an EQE of 0.05% and maximum radiance of 60 mW Sr^{-1} m^{-2} were observed.

Table 3 Photophysical and EL properties of BT-containing transition metal complexes

	λ_{PL} (nm)	λ_{EL} (nm)	CE_{max} (cd A^{-1})	PE_{max} (lm W^{-1})	EQE_{max} (%)	Ref.
75	643	–	–	–	–	[111]
76	643	–	–	–	–	[111]
77	759	432/625/759	–	–	0.16	[112]
78	643	780	–	–	0.02	[111]
79	697	703	–	–	0.88	[113]
80	657	626/766	0.16	0.05	0.13	[114]
81	739	645/761	0.04	0.01	0.04	[114]
82	761	560/826	0.51	0.22	0.49	[114]
83	590	571	0.62	0.22	0.22	[114]

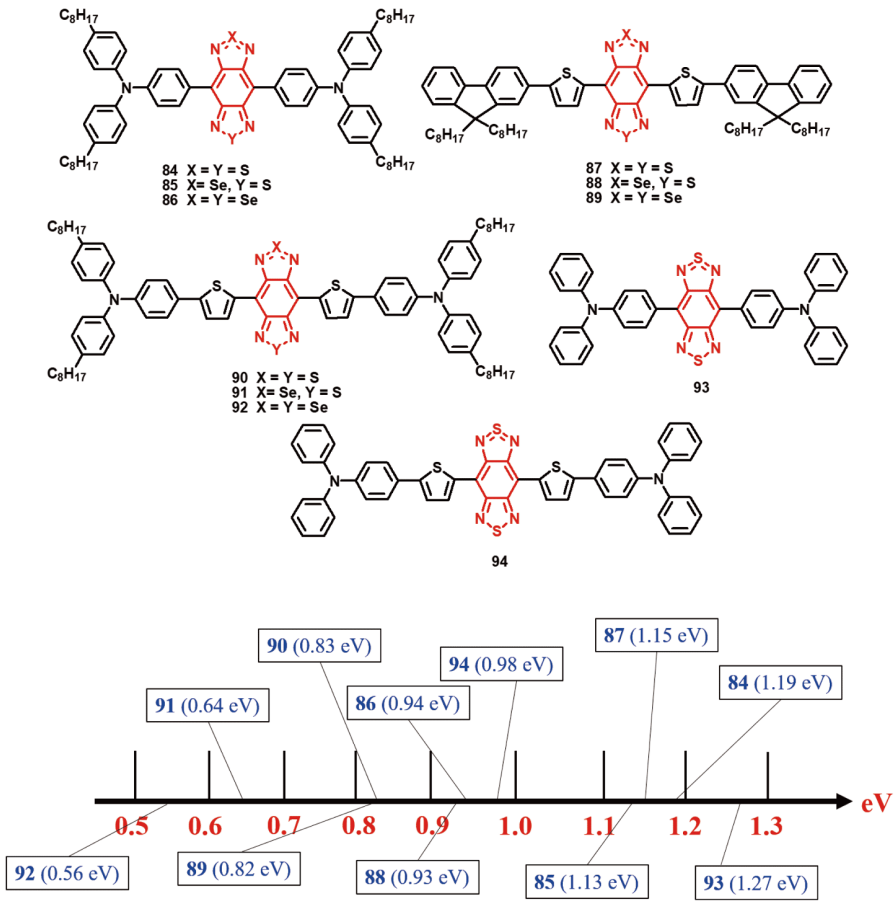

Figure 18 Chemical structures and a wide spectrum of energy gap values (in eV) for **84**–**94** (color online).

Subsequently, through modification of the degree of conjugation and electron-deficient ability of the π-extended BT derivatives, as well as the use of other donor groups, more organic NIR EL materials were designed and synthesized by Wang *et al*. For example, in 2009, NIR fluorescent chromophores based on [1,2,5]thiadiazolo[3,4-*g*]quinoxaline as an electron acceptor and triphenylamine as an electron donor were synthesized and characterized (**95**–**97**, Figure 19) [71]. Their absorption and PL spectra were found to show an obvious red-shift when the π-conjugation of the acceptor unit was increased. The EL spectra of the devices based on these chromophores covered a range in wavelength from 748 to 870 nm and these devices exhibited an EQE of over 1%. In the same year, by choosing benzo[1,2-*c*:4,5-*c*′]bis[(1,2,5) thiadiazole] as an electron acceptor, and slightly modified diphenylamino units as an electron donor, three new NIR organic materials (**98**–**100,** Figure 20) were prepared [70]. Non-doped OLEDs with NIR emission exclusively at 1,080 nm with EQE of 0.28% have been achieved, which represented the best performance at that time. Later, in 2012, they designed and synthesized a family of D-A-D-type NIR fluorophores (**101** and **102,** Figure 20) using [1,2,5]thiadiazolo[3,4-*g*]quinoxaline or benzo[1,2-*c*;4,5-*c*′]bis[1,2,5]thiadiazole as acceptors, and tetraphenylethene as the donor [116]. These emitters exhibited NIR emission in the wavelength range of 600–1,100 nm. Non-doped OLEDs based on these fluorophores were made, which exhibited EL spectra

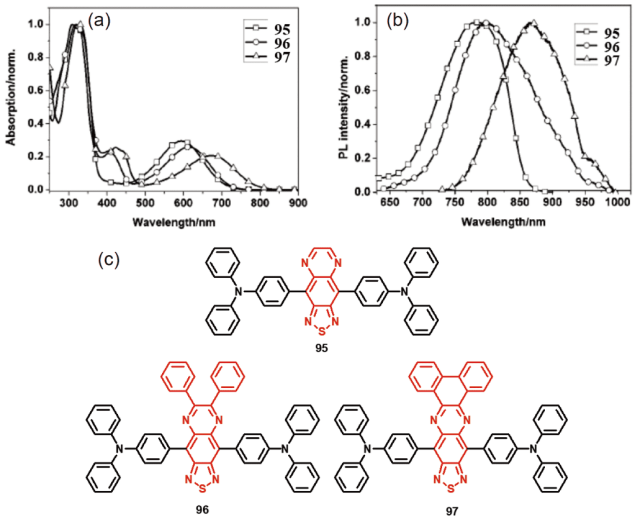

Figure 19 (a) Absorption, (b) PL spectra and (c) chemical structures and of **95**–**97**. Adapted with permission [71]. Copyright 2009, American Chemical Society (color online).

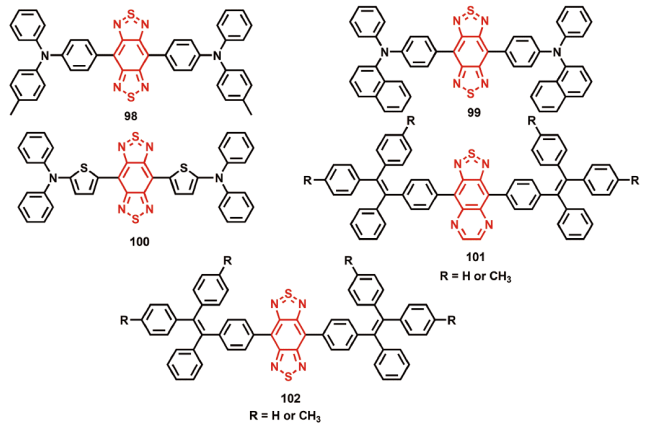

Figure 20 Chemical structures of **98**–**102** (color online).

peaking from 706 to 864 nm with EQE ranging from 0.89% to 0.20%. Their work in designing organic NIR materials based on π-extended BT derivatives has attracted great attention and considerable further investigation by other research groups.

Xue *et al*. [117] synthesized two π-extended BT derivative-based oligomers (**103** and **104**, Figure 21). The energies of the HOMO and LUMO of these oligomers are controlled by the D and A components. Using these oligomers as single emissive layers, EL wavelengths of 692 and 815 nm, as well as EQEs of 1.6% and 3.1% were obtained from their NIR OLEDs. Reynolds *et al*. [118] also designed four π-extended BT-based oligomers (**105**–**108**, Figure 21). The relationship among the spectral, structural and electrochemical properties of these oligomers fully revealed the design rules for organic NIR luminescent materials based on BT or its derivatized heterocycles. Ma and co-workers [119] reported NIR materials based on naphtho[2,3-*c*][1,2,5]thiadiazole as an electron acceptor and TPA as an electron donor (**109**, Figure 21). By incorporating another ancillary acceptor of cyanophenyl group, a red-shift was obtained as compared to its parent NIR emission peak at 710 nm. The non-doped OLED based on the emitter **109** exhibited an excellent NIR emission at 702 nm with a maximum EQE of 1.2%. Furthermore, by using this largely conjugated acceptor unit, they developed another three emitters of **110**–**112** with TPA as the donor group. All of these emitters can emit DR/NIR emission and exhibit HLCT properties. The related devices showed EL wavelengths of 664, 666 and 665 nm, as well as EQEs of 2.8%, 5.06% and 5.35%, respectively [94,120]. In addition, Yang and co-workers [121,122] also designed two NIR

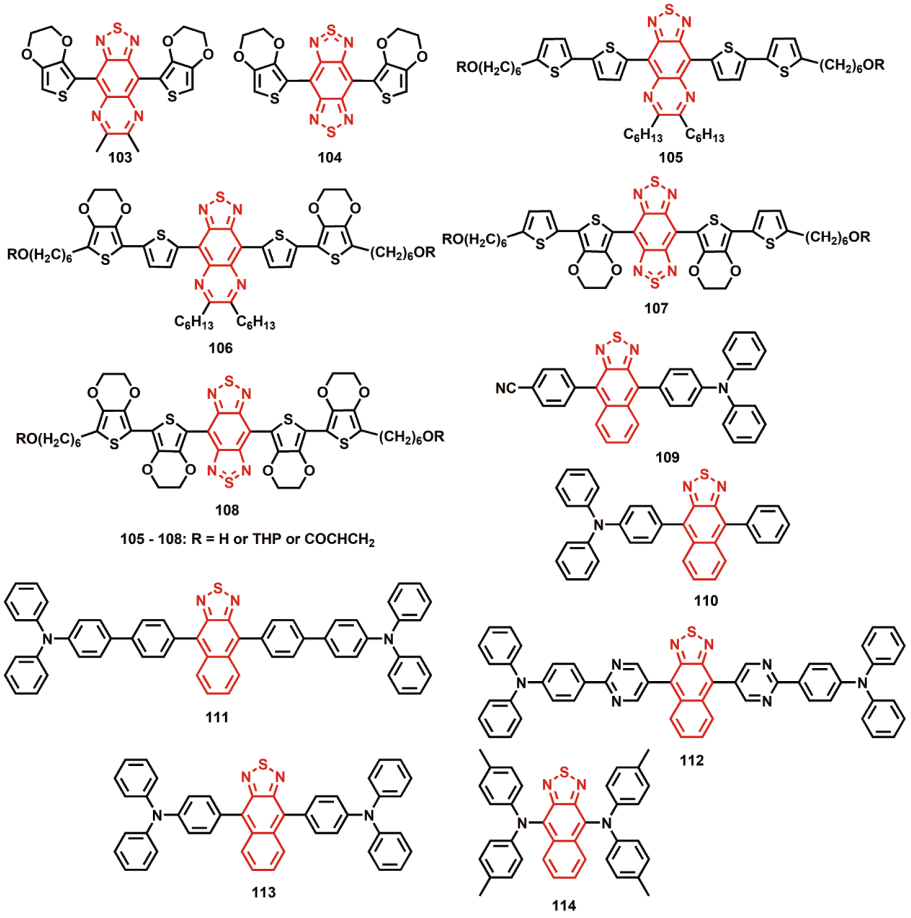

Figure 21 Chemical structures of **103**–**114** (color online).

emissive materials (**113** and **114**, Figure 21) using naphtho-[2,3-*c*][1,2,5]thiadiazole as an electron acceptor and TPA or di(*p*-tolyl)amine as the electron donor. The NIR OLEDs based on **113** and **114** emitters showed excellent EL performance with emission peaks at 696 and 786 nm, as well as EQE of 3.9% and 0.77%, respectively.

π-Extended BT derivative-based copolymers can also be applied as NIR EL materials. Wang and co-workers [123] reported a series of NIR emitting copolymers (**115**, Figure 22), based on a low band gap fluorophore copolymerized with a high-band-gap host backbone. By regulating the ratio of polymerizable monomers, the copolymers with different degrees of polymerization were obtained with different optoelectronic performance. Using these copolymers as the emissive layers, NIR OLEDs emitted different EL emission peaks within 690–930 nm and EQEs of 0.04%–0.36% were obtained. Table 4 summarizes the photophysical and EL properties of π-extended BT derivatives.

4 Summary and outlook

Organic luminescent materials have attracted considerable interest because of their excellent potential in electronic devices, chemical detectors, fluorescent probes and so on. It is important to obtain fluorescent materials with high luminous efficiency through molecular design. More and more efficient EL molecules have been developed successively. However, many new challenges remain to be met for a variety of needs. For example, due to the complex molecular structure, most of the high-efficiency luminescent materials are still in the laboratory-scale research stage and cannot be mass-produced.

This review summarizes the advances in EL materials based on BT acceptor units and its derivatives, including the chemical preparation of materials and their EL performance. Due to their strong ability for electron withdrawal, construction of molecules with the unit core of BT and its derivatives can usually improve the resulting electronic properties. In addition, by modifying the structure of BT, such as by introducing electron-donating or electron-withdrawing groups, and expanding the conjugated structure of the unit, the electronic properties of the materials can be effectively regulated. Based on these methods, EL materials developed based on these units can emit light from visible to NIR, as well as white emission. However, there are also problems with those molecules based on BT derivatives. For example, due to their good planarity and strong electron-withdrawing property, the HOMO and LUMO of the resulting molecules are not well separated, which can always cause large ΔE_{ST}, and the utilization efficiency of triplet excitons is low. Furthermore, π-extended BT derivatives typically have a higher degree of conjugation and largely

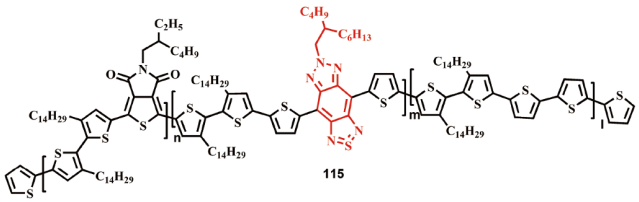

Figure 22 Chemical structure of **115** (color online).

Table 4 Photophysical and EL properties of π-extended BT derivatives

	λ_{PL} (nm)	λ_{EL} (nm)	EQE_{max} (%)	Ref.
84	1065	–	–	[115]
85	1120	–	–	[115]
86	1230	–	–	[115]
87	1055	–	–	[115]
88	1120	–	–	[115]
89	1285	–	–	[115]
90	1125	–	–	[115]
91	1295	–	–	[115]
92	1360	–	–	[115]
93	975	1050	0.05	[115]
94	1120	1115	–	[115]
95	784	752	1.12	[71]
96	800	748	1.20	[71]
97	768	823	0.27	[71]
98	1080	1080	0.73	[70]
99	1040	1050	0.33	[70]
100	1285	1220	–	[70]
101	700/780	706/749	0.89/0.29	[116]
102	787/857	802/864	0.43/0.20	[116]
103	698	692	3.1	[117]
104	805	815	1.5	[117]
105	900	–	–	[118]
106	974	–	–	[118]
107	1020	–	–	[118]
108	1088	–	–	[118]
109	710	702	1.2	[119]
110	687/668	664	2.8	[94]
111	675	665	5.35	[120]
112	676	666	5.06	[120]
113	683	696	3.9	[121]
114	785	786	0.77	[122]
115	700–900	680–930	0.004–0.49	[123]

planar structure, which would give rise to low solubility for the resulting molecules. Generally, introduction of long alkyl chains can increase the solubility, but it also increases the vibration factors and enhances the non-radiative transition, which reduces the internal quantum efficiency.

Except for the molecular structure, the configuration of the fabricated devices also has a great influence on the final performance. Therefore, the optimization of device fabrica-

tion process is particularly important. All in all, the excellent device performance requires the joint efforts of material chemists and device engineers.

Acknowledgements This work was supported by the Science, Technology and Innovation Committee of Shenzhen Municipality (JCYJ20180507183413211), the National Natural Science Foundation of China (51873176, 51903157, 21828102), Hong Kong Research Grants Council (PolyU153058/19P, C6009-17G), Hong Kong Polytechnic University (1-ZE1C), the Endowed Professorship in Energy from Ms Clarea Au (847S), Research Institute for Smart Energy (RISE), and China Postdoctoral Science Foundation Funded Project (2017M622748, 2019T120747). P. Qian also thanks the Foundation of Wenzhou Science & Technology Bureau (W20170003).

Conflict of interest The authors declare no conflict of interest.

1 Wang ZY. *Near-infrared Organic Materials and Emerging Applications*. Boca Raton: CRC Press, 2013
2 Qian G, Wang ZY. *Chem Asian J*, 2010, 5: 1006–1029
3 Zhang Y, Wang Y, Song J, Qu J, Li B, Zhu W, Wong WY. *Adv Opt Mater*, 2018, 6: 1800466
4 Xiang H, Cheng J, Ma X, Zhou X, Chruma JJ. *Chem Soc Rev*, 2013, 42: 6128–6185
5 Wang E, Hou L, Wang Z, Hellstrom S, Mammo W, Zhang F, Inganas O, Andersson MR. *Org Lett*, 2010, 12: 4470–4473
6 Zhang Y, Bao X, Xiao M, Tan H, Tao Q, Wang Y, Liu Y, Yang R, Zhu W. *J Mater Chem A*, 2015, 3: 886–893
7 Liu T, Zhu L, Gong S, Zhong C, Xie G, Mao E, Fang J, Ma D, Yang C. *Adv Opt Mater*, 2017, 5: 1700145
8 Wang S, Yan X, Cheng Z, Zhang H, Liu Y, Wang Y. *Angew Chem Int Ed*, 2015, 54: 13068–13072
9 Yuan Y, Hu Y, Zhang YX, Lin JD, Wang YK, Jiang ZQ, Liao LS, Lee ST. *Adv Funct Mater*, 2017, 27: 1700986
10 Wang B, Wang Y, Hua J, Jiang Y, Huang J, Qian S, Tian H. *Chem Eur J*, 2011, 17: 2647–2655
11 Bis JA, Vishweshwar P, Weyna D, Zaworotko MJ. *Mol Pharm*, 2007, 4: 401–416
12 Pond SJK, Rumi M, Levin MD, Parker TC, Beljonne D, Day MW, Brédas JL, Marder SR, Perry JW. *J Phys Chem A*, 2002, 106: 11470–11480
13 de Melo CEA, Nandi LG, Domínguez M, Rezende MC, Machado VG. *J Phys Org Chem*, 2015, 28: 250–260
14 Albert IDL, Marks TJ, Ratner MA. *J Am Chem Soc*, 1997, 119: 6575–6582
15 Qian Y, Xiao G, Wang G, Lin B, Cui Y, Sun Y. *Dyes Pigments*, 2007, 75: 218–224
16 Liu G, Zhang B, Chen Y, Zhu CX, Zeng L, Siu-Hung Chan D, Neoh KG, Chen J, Kang ET. *J Mater Chem*, 2011, 21: 6027
17 Kim HG, Kim M, Clement JA, Lee J, Shin J, Hwang H, Sin DH, Cho K. *Chem Mater*, 2015, 27: 6858–6868
18 Cui C, Wong WY. *Macromol Rapid Commun*, 2016, 37: 287–302
19 Dou C, Long X, Ding Z, Xie Z, Liu J, Wang L. *Angew Chem Int Ed*, 2016, 55: 1436–1440
20 Bürgi L, Turbiez M, Pfeiffer R, Bienewald F, Kirner HJ, Winnewisser C. *Adv Mater*, 2008, 20: 2217–2224
21 Allard S, Forster M, Souharce B, Thiem H, Scherf U. *Angew Chem*, 2008, 120: 4138–4167
22 Lei T, Wang JY, Pei J. *Acc Chem Res*, 2014, 47: 1117–1126
23 Li Y. *Acc Chem Res*, 2012, 45: 723–733
24 Zhou P, Zhang ZG, Li Y, Chen X, Qin J. *Chem Mater*, 2014, 26: 3495–3501
25 Takimiya K, Osaka I, Nakano M. *Chem Mater*, 2013, 26: 587–593
26 Guo X, Facchetti A, Marks TJ. *Chem Rev*, 2014, 114: 8943–9021
27 Cheng YJ, Yang SH, Hsu CS. *Chem Rev*, 2009, 109: 5868–5923
28 Guo X, Xin H, Kim FS, Liyanage ADT, Jenekhe SA, Watson MD. *Macromolecules*, 2011, 44: 269–277
29 Wang M, Hu X, Liu P, Li W, Gong X, Huang F, Cao Y. *J Am Chem Soc*, 2011, 133: 9638–9641
30 Parker TC, Patel DGD, Moudgil K, Barlow S, Risko C, Brédas JL, Reynolds JR, Marder SR. *Mater Horiz*, 2015, 2: 22–36
31 Zhang M, Tsao HN, Pisula W, Yang C, Mishra AK, Müllen K. *J Am Chem Soc*, 2007, 129: 3472–3473
32 Zhou E, Cong J, Yamakawa S, Wei Q, Nakamura M, Tajima K, Yang C, Hashimoto K. *Macromolecules*, 2010, 43: 2873–2879
33 Neto BAD, Lapis AAM, da Silva Júnior EN, Dupont J. *Eur J Org Chem*, 2013, 2013: 228–255
34 Tan SE, Sarjadi MS. *Polym Sci Ser B*, 2017, 59: 479–496
35 Yu J, Tan H, Meng F, Lv K, Zhu W, Su S. *Dyes Pigments*, 2016, 131: 231–238
36 Xiao B, Tang A, Zhang J, Mahmood A, Wei Z, Zhou E. *Adv Energy Mater*, 2017, 7: 1602269
37 Tang A, Xiao B, Chen F, Zhang J, Wei Z, Zhou E. *Adv Energy Mater*, 2018, 8: 1801582
38 Lee J, Park HJ, Joo JM, Hwang DH. *Macromol Res*, 2019, 27: 115–118
39 Data P, Kurowska A, Pluczyk S, Zassowski P, Pander P, Jedrysiak R, Czwartosz M, Otulakowski L, Suwinski J, Lapkowski M, Monkman AP. *J Phys Chem C*, 2016, 120: 2070–2078
40 Wu XF, Fu WF, Xu Z, Shi M, Liu F, Chen HZ, Wan JH, Russell TP. *Adv Funct Mater*, 2015, 25: 5954–5966
41 Tang A, Zhan C, Yao J, Zhou E. *Adv Mater*, 2017, 29: 1600013
42 Liu C, Dong S, Cai P, Liu P, Liu S, Chen J, Liu F, Ying L, Russell TP, Huang F, Cao Y. *ACS Appl Mater Interfaces*, 2015, 7: 9038–9051
43 Lei T, Lai YC, Hong G, Wang H, Hayoz P, Weitz RT, Chen C, Dai H, Bao Z. *Small*, 2015, 11: 2946–2954
44 Ganguly A, Zhu J, Kelly TL. *J Phys Chem C*, 2017, 121: 9110–9119
45 Lu Q, Cai W, Zhang X, Yang C, Ge H, Chen Y, Niu H, Wang W. *Eur Polym J*, 2018, 108: 124–137
46 Jiang Y, Gao Y, Tian H, Ding J, Yan D, Geng Y, Wang F. *Macromolecules*, 2016, 49: 2135–2144
47 Wang JT, Takashima S, Wu HC, Chiu YC, Chen Y, Isono T, Kakuchi T, Satoh T, Chen WC. *Adv Funct Mater*, 2016, 26: 2695–2705
48 Liu J, Zhou Q , Cheng Y , Geng Y , Wang L , Ma D , Jing X , Wang F . *Adv Funct Mater*, 2006, 16: 957–965
49 Chen L, Li P, Cheng Y, Xie Z, Wang L, Jing X, Wang F. *Adv Mater*, 2011, 23: 2986–2990
50 Liu J, Chen L, Shao S, Xie Z, Cheng Y, Geng Y, Wang L, Jing X, Wang F. *J Mater Chem*, 2008, 18: 319–327
51 Ku SY, Chi LC, Hung WY, Yang SW, Tsai TC, Wong KT, Chen YH, Wu CI. *J Mater Chem*, 2009, 19: 773–780
52 Zhang J, Chen W, Rojas AJ, Jucov EV, Timofeeva TV, Parker TC, Barlow S, Marder SR. *J Am Chem Soc*, 2013, 135: 16376–16379
53 Sanzone A, Calascibetta A, Ghiglietti E, Ceriani C, Mattioli G, Mattiello S, Sassi M, Beverina L. *J Org Chem*, 2018, 83: 15029–15042
54 Wang X, Wang M. *Polym Chem*, 2014, 5: 5784–5792
55 Cao Q, Howard JL, Wheatley E, Browne DL. *Angew Chem Int Ed*, 2018, 57: 11339–11343
56 Heiskanen JP, Vivo P, Saari NM, Hukka TI, Kastinen T, Kaunisto K, Lemmetyinen HJ, Hormi OEO. *J Org Chem*, 2016, 81: 1535–1546
57 Roy C, Bura T, Beaupré S, Légaré MA, Sun JP, Hill IG, Leclerc M. *Macromolecules*, 2017, 50: 4658–4667
58 Mancilha FS, DaSilveira Neto BA, Lopes AS, Moreira PF, Quina FH, Gonçalves RS, Dupont J. *Eur J Org Chem*, 2006, 2006: 4924–4933
59 Jin Y, Kim Y, Kim SH, Song S, Woo HY, Lee K, Suh H. *Macromolecules*, 2008, 41: 5548–5554
60 Speros JC, Paulsen BD, Slowinski BS, Frisbie CD, Hillmyer MA. *ACS Macro Lett*, 2012, 1: 986–990

61 Hassan Omar O, la Gatta S, Tangorra RR, Milano F, Ragni R, Operamolla A, Argazzi R, Chiorboli C, Agostiano A, Trotta M, Farinola GM. *Bioconjugate Chem*, 2016, 27: 1614–1623
62 Wang T, Scarratt NW, Yi H, Coleman IF, Zhang Y, Grant RT, Yao J, Skoda MWA, Dunbar ADF, Jones RAL, Iraqi A, Lidzey DG. *J Mater Chem C*, 2015, 3: 4007–4015
63 Lee J, Malekshahi Byranvand M, Kang G, Son SY, Song S, Kim GW, Park T. *J Am Chem Soc*, 2017, 139: 12175–12181
64 Livi F, Zawacka NK, Angmo D, Jørgensen M, Krebs FC, Bundgaard E. *Macromolecules*, 2015, 48: 3481–3492
65 Wudarczyk J, Papamokos G, Marszalek T, Nevolianis T, Schollmeyer D, Pisula W, Floudas G, Baumgarten M, Müllen K. *ACS Appl Mater Interfaces*, 2017, 9: 20527–20535
66 Oosterhout SD, Savikhin V, Zhang J, Zhang Y, Burgers MA, Marder SR, Bazan GC, Toney MF. *Chem Mater*, 2017, 29: 3062–3069
67 Hasegawa T, Ashizawa M, Aoyagi K, Masunaga H, Hikima T, Matsumoto H. *Org Lett*, 2017, 19: 3275–3278
68 Cai T, Zhou Y, Wang E, Hellström S, Zhang F, Xu S, Inganäs O, Andersson MR. *Sol Energy Mater Sol Cells*, 2010, 94: 1275–1281
69 Kavak E, Us CN, Yavuz E, Kivrak A, İçli Özkut M. *Electrochim Acta*, 2015, 182: 537–543
70 Qian G, Zhong Z, Luo M, Yu D, Zhang Z, Wang ZY, Ma D. *Adv Mater*, 2009, 21: 111–116
71 Qian G, Zhong Z, Luo M, Yu D, Zhang Z, Ma D, Wang ZY. *J Phys Chem C*, 2009, 113: 1589–1595
72 Yen YS, Ni JS, Hung WI, Hsu CY, Chou HH, Lin JTS. *ACS Appl Mater Interfaces*, 2016, 8: 6117–6126
73 Oliveira FFD, Santos DCBD, Lapis AAM, Corrêa JR, Gomes AF, Gozzo FC, Moreira Jr. PF, de Oliveira VC, Quina FH, Neto BAD. *BioOrg Medicinal Chem Lett*, 2010, 20: 6001–6007
74 da Cruz EHG, Carvalho PHPR, Corrêa JR, Silva DAC, Diogo EBT, de Souza Filho JD, Cavalcanti BC, Pessoa C, de Oliveira HCB, Guido BC, da Silva Filho DA, Neto BAD, da Silva Júnior EN. *New J Chem*, 2014, 38: 2569
75 Sun X, Xu X, Qiu W, Yu G, Zhang H, Gao X, Chen S, Song Y, Liu Y. *J Mater Chem*, 2008, 18: 2709
76 Yang Y, Zhou Y, He Q, He C, Yang C, Bai F, Li Y. *J Phys Chem B*, 2009, 113: 7745–7752
77 Zhang J, Yang Y, He C, Li YF. *Sci China Chem*, 2011, 54: 695–698
78 Zhao Z, Deng C, Chen S, Lam JWY, Qin W, Lu P, Wang Z, Kwok HS, Ma Y, Qiu H, Tang BZ. *Chem Commun*, 2011, 47: 8847–8849
79 Li Y, Wang W, Zhuang Z, Wang Z, Lin G, Shen P, Chen S, Zhao Z, Tang BZ. *J Mater Chem C*, 2018, 6: 5900–5907
80 Lee WWH, Zhao Z, Cai Y, Xu Z, Yu Y, Xiong Y, Kwok RTK, Chen Y, Leung NLC, Ma D, Lam JWY, Qin A, Tang BZ. *Chem Sci*, 2018, 9: 6118–6125
81 Chen S, Kwok HS. *Org Electron*, 2011, 12: 677–681
82 Thangthong A, Prachumrak N, Sudyoadsuk T, Namuangruk S, Keawin T, Jungsuttiwong S, Kungwan N, Promarak V. *Org Electron*, 2015, 21: 117–125
83 Angioni E, Chapran M, Ivaniuk K, Kostiv N, Cherpak V, Stakhira P, Lazauskas A, Tamulevičius S, Volyniuk D, Findlay NJ, Tuttle T, Grazulevicius JV, Skabara PJ. *J Mater Chem C*, 2016, 4: 3851–3856
84 Pathak A, Justin Thomas KR, Singh M, Jou JH. *J Org Chem*, 2017, 82: 11512–11523
85 Peng Z, Zhang K, Huang Z, Wang Z, Duttwyler S, Wang Y, Lu P. *J Mater Chem C*, 2019, 7: 2430–2435
86 Fell VHK, Findlay NJ, Breig B, Forbes C, Inigo AR, Cameron J, Kanibolotsky AL, Skabara PJ. *J Mater Chem C*, 2019, 7: 3934–3944
87 Guo J, Li XL, Nie H, Luo W, Gan S, Hu S, Hu R, Qin A, Zhao Z, Su SJ, Tang BZ. *Adv Funct Mater*, 2017, 27: 1606458
88 Wong MY, Zysman-Colman E. *Adv Mater*, 2017, 29: 1605444
89 Liu B, Yu ZW, He D, Zhu ZL, Zheng J, Yu YD, Xie WF, Tong QX, Lee CS. *J Mater Chem C*, 2017, 5: 5402–5410
90 Chen WC, Yuan Y, Ni SF, Tong QX, Wong FL, Lee CS. *Chem Sci*, 2017, 8: 3599–3608
91 Xue J, Liang Q, Zhang Y, Zhang R, Duan L, Qiao J. *Adv Funct Mater*, 2017, 27: 1703283
92 Ni F, Wu Z, Zhu Z, Chen T, Wu K, Zhong C, An K, Wei D, Ma D, Yang C. *J Mater Chem C*, 2017, 5: 1363–1368
93 Yao L, Zhang S, Wang R, Li W, Shen F, Yang B, Ma Y. *Angew Chem Int Ed*, 2014, 53: 2119–2123
94 Li W, Pan Y, Yao L, Liu H, Zhang S, Wang C, Shen F, Lu P, Yang B, Ma Y. *Adv Opt Mater*, 2014, 2: 892–901
95 Chen X, Yang Z, Li W, Mao Z, Zhao J, Zhang Y, Wu YC, Jiao S, Liu Y, Chi Z. *ACS Appl Mater Interfaces*, 2019, 11: 39026–39034
96 Xie W, Li B, Cai X, Li M, Qiao Z, Tang X, Liu K, Gu C, Ma Y, Su SJ. *Front Chem*, 2019, 7: 276
97 Zhang Y, Zhou X, Zhou C, Su Q, Chen S, Song J, Wong WY. *J Mater Chem C*, 2020, 8: 6851–6860
98 Xu Y, Guan R, Jiang J, Yang W, Zhen H, Peng J, Cao Y. *J Polym Sci A Polym Chem*, 2008, 46: 453–463
99 Chen Q, Liu N, Ying L, Yang W, Wu H, Xu W, Cao Y. *Polymer*, 2009, 50: 1430–1437
100 Wang H, Xu Y, Tsuboi T, Xu H, Wu Y, Zhang Z, Miao Y, Hao Y, Liu X, Xu B, Huang W. *Org Electron*, 2013, 14: 827–838
101 Nagaraju S, Ravindran E, Varathan E, Subramanian V, Somanathan N. *RSC Adv*, 2016, 6: 92778–92785
102 Jiu Y, Wang J, Liu C, Lai W, Zhao L, Li X, Jiang Y, Xu W, Zhang X, Huang W. *Chin J Chem*, 2015, 33: 873–880
103 Jiu YD, Liu CF, Wang JY, Lai WY, Jiang Y, Xu WD, Zhang XW, Huang W. *Polym Chem*, 2015, 6: 8019–8028
104 Jiu Y, Wang J, Yi J, Liu CF, Zhang XW, Lai WY, Huang W. *Polym Chem*, 2017, 8: 851–859
105 Liu Z, Fang C, Cai X, Gao X, Li P, Zhang Q, Tu G. *Dyes Pigments*, 2018, 156: 39–44
106 Mishra SP, Palai AK, Srivastava R, Kamalasanan MN, Patri M. *J Polym Sci A Polym Chem*, 2009, 47: 6514–6525
107 Qu B, Feng L, Yang H, Gao Z, Gao C, Chen Z, Xiao L, Gong Q. *Synth Met*, 2012, 162: 1587–1593
108 Demir N, Oner I, Varlikli C, Ozsoy C, Zafer C. *Thin Solid Films*, 2015, 589: 153–160
109 Ahn HI, Moon JS, Kim WG, Uddin MA, Choi J, Kim C, Woo HY, Kim N, Oh JW. *Org Electron*, 2015, 25: 206–211
110 Krucaite G, Tavgeniene D, Xie Z, Lin X, Zhang B, Grigalevicius S. *Optical Mater*, 2018, 76: 63–68
111 Zhang YM, Meng F, Tang JH, Wang Y, You C, Tan H, Liu Y, Zhong YW, Su S, Zhu W. *Dalton Trans*, 2016, 45: 5071–5080
112 Yu J, He K, Li Y, Tan H, Zhu M, Wang Y, Liu Y, Zhu W, Wu H. *Dyes Pigments*, 2014, 107: 146–152
113 Zhang Y, Yin Z, Meng F, Yu J, You C, Yang S, Tan H, Zhu W, Su S. *Org Electron*, 2017, 50: 317–324
114 Zhang Y, Chen Z, Wang X, He J, Wu J, Liu H, Song J, Qu J, Chan WTK, Wong WY. *Inorg Chem*, 2018, 57: 14208–14217
115 Qian G, Dai B, Luo M, Yu D, Zhan J, Zhang Z, Ma D, Wang ZY. *Chem Mater*, 2008, 20: 6208–6216
116 Du X, Qi J, Zhang Z, Ma D, Wang ZY. *Chem Mater*, 2012, 24: 2178–2185
117 Yang Y, Farley RT, Steckler TT, Eom SH, Reynolds JR, Schanze KS, Xue J. *J Appl Phys*, 2009, 106: 044509
118 Ellinger S, Graham KR, Shi P, Farley RT, Steckler TT, Brookins RN, Taranekar P, Mei J, Padilha LA, Ensley TR, Hu H, Webster S, Hagan DJ, Van Stryland EW, Schanze KS, Reynolds JR. *Chem Mater*, 2011, 23: 3805–3817
119 Tang X, Li XL, Liu H, Gao Y, Shen Y, Zhang S, Lu P, Yang B, Su SJ, Ma Y. *Dyes Pigments*, 2018, 149: 430–436
120 Li Y, Yao J, Wang C, Zhou X, Xu Y, Hanif M, Qiu X, Hu D, Ma D, Ma Y. *Dyes Pigments*, 2020, 173: 107960
121 Liu T, Zhu L, Zhong C, Xie G, Gong S, Fang J, Ma D, Yang C. *Adv Funct Mater*, 2017, 27: 1606384
122 Liu T, Xie G, Zhong C, Gong S, Yang C. *Adv Funct Mater*, 2018, 28: 1706088
123 Murto P, Minotto A, Zampetti A, Xu X, Andersson MR, Cacialli F, Wang E. *Adv Opt Mater*, 2016, 4: 2068–2076